



LAWRENCE  
LIVERMORE  
NATIONAL  
LABORATORY

# Rapid dissolution by laser driven hydrothermal processing (LDHP) of basalt geostandards

C. B. Durrant, G. A. Brennecka, J. Wimpenny, D. G. Weisz, R. Mariella

July 29, 2021

Journal of Laser Applications

## **Disclaimer**

---

This document was prepared as an account of work sponsored by an agency of the United States government. Neither the United States government nor Lawrence Livermore National Security, LLC, nor any of their employees makes any warranty, expressed or implied, or assumes any legal liability or responsibility for the accuracy, completeness, or usefulness of any information, apparatus, product, or process disclosed, or represents that its use would not infringe privately owned rights. Reference herein to any specific commercial product, process, or service by trade name, trademark, manufacturer, or otherwise does not necessarily constitute or imply its endorsement, recommendation, or favoring by the United States government or Lawrence Livermore National Security, LLC. The views and opinions of authors expressed herein do not necessarily state or reflect those of the United States government or Lawrence Livermore National Security, LLC, and shall not be used for advertising or product endorsement purposes.

1 **Rapid dissolution without elemental fractionation by laser driven hydrothermal processing**  
2 **(LDHP)**

3  
4 Chad B. Durrant,<sup>1</sup> Gregory A. Brennecka,<sup>\*1</sup> Josh Wimpenny,<sup>1</sup> David G. Weisz,<sup>1</sup> Raymond  
5 Mariella, Jr.<sup>1</sup>

6  
7 <sup>1</sup>Lawrence Livermore National Laboratory, Livermore, California 94550, USA

8 \*Corresponding author

9  
10 **ABSTRACT**

11  
12 Traditional dissolution of geologic samples often requires a significant time investment. Here we  
13 present an alternative method for the dissolution of geologic materials using laser driven  
14 hydrothermal processing (LDHP). LDHP uses laser energy directed onto a submerged sample,  
15 which increases the temperature and pressure at the liquid-sample interface and drives the  
16 hydrothermal dissolution coupled with photomechanical spallation, an ablative process. This  
17 uses focused 527 nm laser energy at 40 W average power, 1 kHz pulse repetition rate and 115 ns  
18 pulse duration. When LDHP is performed on basalt geostandards (BCR-2 and BHVO-2) using  
19 the conditions outlined, we show that LDHP does not produce significant elemental fractionation  
20 and thus can be considered an alternative processing method to traditional mechanical crushing  
21 and acid digestion. Additionally, it is possible using LDHP to utilize the spatially confined beam  
22 to target and selectively isolate individual phases in a rock, potentially alleviating the need for  
23 mechanical separation of inclusions that are difficult to physically isolate. Furthermore, using  
24 this outlined method of LDHP, we demonstrate full dissolution of 120 mg of obsidian in 85  
25 minutes, meaning that LDHP is a potentially very useful method when sample processing is time  
26 sensitive.

27  
28  
29 **Keywords**

30  
31 Laser Driven Hydrothermal Process (LDHP), Dissolution, Comminution, Elemental Fractionation,  
32 Laser Ablation in Liquid (LAL)

33  
34  
35 **1. Introduction**

36  
37 The bulk dissolution of rocks, sediments, and /or minerals is a key prerequisite for many types of  
38 geochemical analyses. However, the procedures that are typically used to fully digest samples  
39 can be time-consuming, particularly for samples containing silicate minerals, and can introduce  
40 higher backgrounds depending on the volume of reagents used. Most methods require the sample  
41 to be crushed to maximize the surface area in contact with caustic mineral acids that include  
42 concentrated nitric, hydrochloric, and hydrofluoric acids. The full dissolution procedure can  
43 involve several days of heating with a variety of acid combinations, depending on the sample  
44 matrix and mass being dissolved [1-4]. Only once dissolution is achieved can the sample then be  
45 diluted and introduced to analytical techniques such as inductively coupled plasma mass

46 spectrometry (ICP-MS) or, in many cases, processed through chemical procedures designed to  
47 isolate desired elements prior to isotopic analysis.

48  
49 Because traditional techniques to dissolve geological samples can be time consuming, this can be  
50 particularly problematic if analyses are time sensitive or high sample throughput is desired. In  
51 addition, bulk dissolution techniques are not always suitable when a particular mineral phase is  
52 of interest. In this case the targeted mineral or portion of the rock must be mechanically removed  
53 by procedures such as mineral picking or magnetic separation [e.g., 5], which adds further  
54 processing time. *In-situ* techniques such as laser ablation ICP-MS can sometimes be used in  
55 these cases, but are not suitable for all elements and/or isotope systems. For cases where  
56 throughput is a concern and/or a more targeted dissolution procedure is required, we have  
57 developed a new dissolution method termed laser-driven hydrothermal processing (LDHP).

58  
59 Laser ablation in liquid (LAL) processes have rapidly developed over the last two decades.  
60 LDHP is an LAL method of processing material with laser energy, wherein a sample is  
61 submerged in liquid—either water or acid—and laser energy is directed onto the submerged  
62 sample. Whereas most LAL processes utilize short pulses (femtosecond to a few nanoseconds)  
63 and effect the creation of plasma in the materials [6-9], the laser energy in LDHP is deposited  
64 into the sample over a relatively longer time period (100-300 ns), causing a directed temperature  
65 increase and tensile stresses that reflect from the sample surface and can lead to fracturing at the  
66 liquid-sample interface [5]. Unlike most LAL processes, LDHP does not result in plasma  
67 formation. During LDHP the increased temperature and pressure of the liquid at the interface  
68 accelerates the hydrothermal processing of the material [7]. Previous work has shown that this  
69 process results in a transient dissolution of the wetted surface material until cessation of the laser  
70 pulsing. After cessation, some of the transiently dissolved SiO<sub>2</sub> re-forms along the surface [8].  
71 During LDHP, the reflected tensile stress will sometimes result in spallation from the surface of  
72 the sample [10-12], where small, ejected pieces remain undissolved. Because of the resulting  
73 undissolved particles, full dissolution does not happen using only laser pulses. For this reason, it  
74 is best to follow LDHP with acidification and heat to complete the dissolution process. This  
75 acidification step involves adding a few milliliters of concentrated nitric and hydrofluoric acid  
76 while heating the solution.

77  
78 Due to the directed energy pulses and the extreme conditions created locally on the sample  
79 surface, one particular concern using LDHP to process samples, either in bulk or subsamples, is  
80 the potential for elemental fractionation to occur as a result of laser processing. In other words,  
81 does the directed energy of LDHP cause volatile elements to behave differently than refractory  
82 elements during the digestion process? For LDHP to be considered a viable digestion method it  
83 is critical that geologic samples digested by LDHP yield the same results as samples digested by  
84 traditional methods. To this end, we present new major and trace element data for two well-  
85 characterized rock standards (the USGS basalt standards BCR-2 and BHVO-2), with direct  
86 comparison between data obtained by LDHP and data obtained using traditional acid digestion  
87 techniques. We also present the results of a timed test evaluating the speed at which laser-  
88 assisted dissolution occurs.

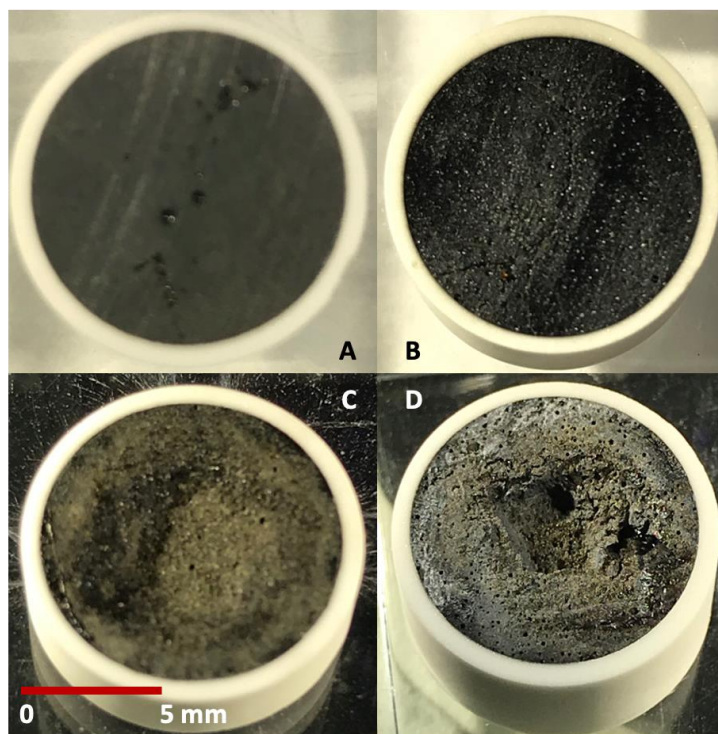
## 90 **2. Materials and methods**

91

92 *2.1 Standards and samples*

93 The basalt standards BCR-2 and BHVO-2 were acquired from the USGS as homogenized  
 94 powders. These geostandards have been used in geochemical studies for decades with the  
 95 compositions available in their certificate of analysis [13, 14]. Because LDHP has not been  
 96 tested on powdered samples, powdered material from each geostandard was fused into 1 to 2 g  
 97 pucks, approximately 1 cm in diameter, within alumina crucibles (see Figure 1) at 1300 °C for  
 98 ~10 minutes and let cool at room temperature. Pieces of the fused samples of each geostandard  
 99 were used as comparison samples, digested by traditional techniques (crushing, followed by  
 100 concentrated HNO<sub>3</sub>, HCl, and HF acids on a hotplate at 120° C) as well as processed by LDHP.  
 101 Approximately equivalent masses of each standard were dissolved for each method (see Table  
 102 1).

103



104

105 *Figure 1. The geostandard samples BHVO-2 and BCR-2 prior to laser processing are shown in (A) and (B) respectively. The*  
 106 *post-processed BHVO-2 and BCR-2 samples are shown in (C) and (D) respectively. Approximately 12 mg was processed and*  
 107 *removed from the BCR-2 sample and 15 mg was processed and removed from the BHVO-2 sample.*

108

109 *Table 1. The mass of sample removed by LDHP for each of the geological standards.*

Sample	Mass Removed-LDHP (mg)	Mass Dissolved-traditional (mg)
BCR-2	12.51	16.7
BHVO-2	16.97	19.0

110

111 *2.2 Laser characteristics and operating conditions*

112

113 It has been shown in prior work that LDHP is most effective using modest laser fluences (sub-  
 114 ablation) and long laser pulse durations [8, 15-17]. The laser used in our experiments was a

115 Photonics Industries Nd:YLF (neodymium-doped yttrium lithium fluoride crystal) DM50-527  
116 solid state laser which emits green 527-nm laser light pulses. The operating conditions were 40  
117 W average power, 1 kHz pulse repetition rate with a pulse duration of ~115 ns and a dwell time  
118 (duration of the laser pulses at a single point before moving to the next point in a raster) of 4 ms.  
119 This laser produces a very-high-order Gaussian beam ( $M^2 \approx 13$ ), and with an 18-cm-focal-length  
120 biconvex lens produces a focused-spot shape that is a distorted rectangle.

121

122

### 123 *2.3 Digestion techniques and composition measurements*

124

125 In order to test the LDHP method, corresponding amounts of the fused BHVO-2 and BCR-2  
126 glasses were crushed, weighed, and dissolved using a traditional benchtop acid digestion  
127 procedure. This included a combination of concentrated hydrochloric, nitric, and hydrofluoric  
128 acids (Seastar® grade) and standard 15 mL Savillex® beakers on a hotplate at 120 °C. This  
129 process took well over 24 hrs and multiple dry-downs were required for acid changing.

130

131 Dissolution of the geostandards with LDHP requires a two-step process. First, LDHP with the  
132 laser is used to partially dissolve and finely comminute the sample. Then, since some of the  
133 sample is ejected as small undissolved particles, an acidification and heating step completes the  
134 dissolution of the particulates. Each sample was processed using the laser for 10 minutes in ~40  
135 mL of 18.2 Ω MQ water in a cleaned glass beaker. The supernatant and comminuted residue was  
136 decanted into pre-cleaned 50 mL plastic centrifuge tubes and the samples were rinsed with a few  
137 mL of MQ to collect any remaining particles that may have deposited on the sample surface  
138 during laser firing. The remaining solid geostandards were dried and weighed to determine the  
139 amount of material removed due to laser processing. The sample supernatants were acidified by  
140 adding 2 mL of concentrated nitric acid and 1 mL of hydrofluoric acid, transferred to Savillex®  
141 beakers, capped, and heated to complete the dissolution of fine particulate matter present after  
142 laser processing.

143

144 Following complete dissolution, aliquots of the four samples (designated “Traditional BCR-2”,  
145 “Traditional BHVO-2”, “Laser BCR-2”, and “Laser BHVO-2”) were taken and measured using a  
146 Thermo Element XR ICP-MS to determine the elemental composition of each sample. Samples  
147 were sub-aliquoted, dried, and redissolved in 2% HNO<sub>3</sub> + 0.005M HF for introduction to the  
148 mass spectrometer. Raw intensities were quantified using calibration standard solutions  
149 following previously published techniques at LLNL [18-20]. Long term accuracy of major and  
150 trace element analyses were assessed by repeated analyses of USGS rock standards including  
151 BCR-2 and BHVO-2, with measured concentrations typically accurate to within 10% of  
152 reference values [18-20]. For each sample, 26 elements with a range of geochemical behaviors  
153 were measured compared between the traditional acid digestion and LDHP method to determine  
154 if any systematic differences were observed between the two digestion methods. In addition,  
155 process blanks were measured to determine the trace element contributions from the procedure  
156 and reagents used. These blanks were negligible for all reported elements.

157

158

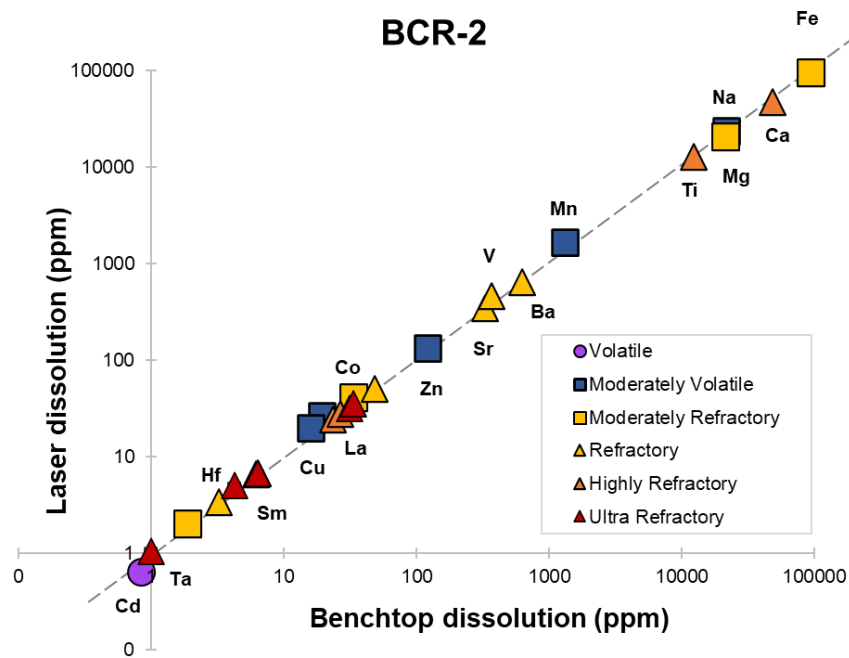
## 159 **3. Results and discussion**

160

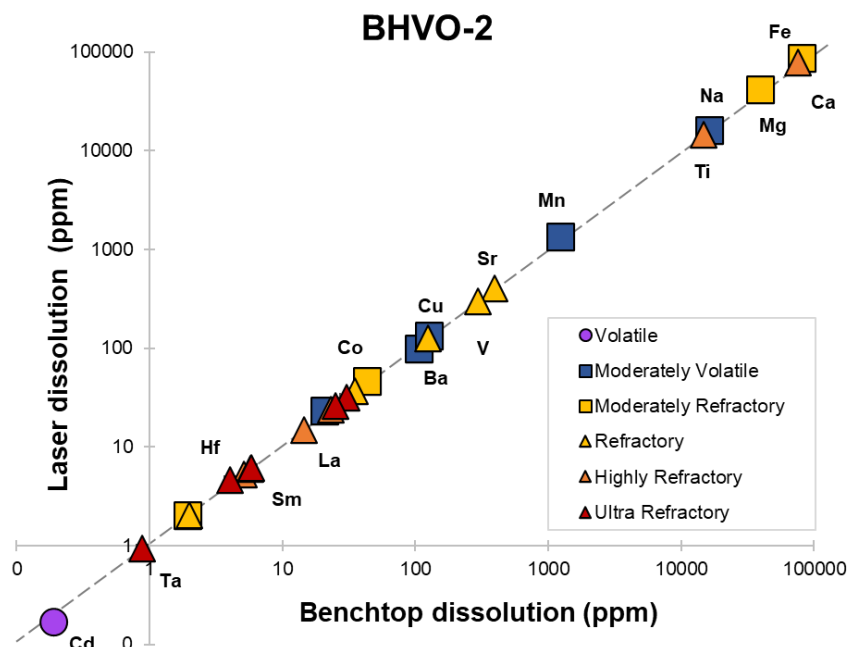
161 3.1 Elemental fractionation?

162 For LDHP to be considered a viable alternative to traditional acid digestion of geologic samples,  
163 it is important that no elemental fractionation occurs during processing. For example, if  
164 volatilization and loss of certain elements occurred during LDHP, it would not be a suitable  
165 alternative for most projects. If, however, LDHP does not chemically fractionate elements during  
166 processing, it could be suitable for a wide array of uses. Figure 2 shows the concentration results  
167 by traditional acid digestion (x-axis) versus LDHP with acidification (y-axis) of BCR-2, and  
168 Figure 3 similarly gives the elemental concentration for both methods for BHVO-2.  
169

170 To compare the trace element compositions measured from both a traditional bench top  
171 dissolution and the laser-assisted dissolution method a 1:1 line is overlaid on both Figures 2 and  
172 3, indicating equivalency. A total of 26 elements were analyzed (Figures 2 and 3, Table 2) and  
173 these were selected based on their variable concentrations and volatilities. The volatility groups  
174 were determined based on work by Lodders [21].  
175



176  
177 Figure 2: A comparison of elemental concentrations obtained by a traditional benchtop dissolution and laser assisted dissolution  
178 of BCR-2. The dashed gray line is a 1:1 line for reference. For clarity, not all elements are labeled. Uncertainties of 10% are  
179 smaller than the symbols.



180

181 *Figure 3. A comparison of elemental concentrations obtained by both a traditional benchtop dissolution and laser assisted*  
 182 *dissolution of BHVO-2. The dashed gray line is a 1:1 line for reference. For clarity, not all elements are labeled. Uncertainties of*  
 183 *10% are smaller than the symbols.*

184 In almost all cases, regardless of the volatility or concentration of the elements, the measured  
 185 concentrations for both standards prepared by both methods were within 10% of the reference  
 186 literature values (Figures 2 and 3; Table 2). The corroboration of elemental concentration across  
 187 the geochemical spectrum, from volatile to highly refractory elements, supports the supposition  
 188 that the method of LDHP used here does not result in elemental fractionation during processing,  
 189 even for highly volatile species.

190

191 *Table 2. Concentration values for the two different methods and reference values for comparison. The uncertainty for each value*  
 192 *in the "Laser-assisted" and "Benchtop" columns is ±10% and is not listed for ease of reading. Condensation phases are based on*  
 193 *50% condensation temperatures [21].*

Condensation Phase	Element	BCR-2 Concentration (ppm)			BHVO-2 Concentration (ppm)		
		Laser-assisted	Benchtop	Reference [13]	Laser-assisted	Benchtop	Reference [14]
Volatile	Cd	0.86	0.63	0.69 ± 0.29 *	0.19	0.17	0.15 ± 0.05 *
Moderately Volatile	Zn	125	129	127 ± 9	107	97.7	103 ± 6
Moderately Volatile	Na	22088	22974	23400 ± 800	16436	15996	16400 ± 600
Moderately Volatile	Ga	19.7	25.9	23 ± 2	21.1	22.9	21.7 ± 0.9
Moderately Volatile	Mn	1354	1625	1520 ± 60	1254	1328	1290 ± 40
Moderately Volatile	Cu	16.4	19.1	19 ± 2	128	133	127 ± 7
Moderately Refractory	Eu	1.9	2.0	2 ± 0.01	2.0	2.0	2.04 ± 0.01 *
Moderately Refractory	Mg	21629	20442	21600 ± 300	39662	41250	43600 ± 700
Moderately Refractory	Fe	95080	93826	96500 ± 1500	82183	85927	86300 ± 1400
Moderately Refractory	Co	33.8	40.7	37 ± 3	43.7	45.4	45 ± 3
Refractory	Sr	331	343	346 ± 14	396	401	389 ± 23
Refractory	Ba	624	649	683 ± 28	124	125	130 ± 13
Refractory	Ce	48.7	51.0	53 ± 2	35.1	36.3	38 ± 2
Refractory	Yb	3.2	3.4	3.5 ± 0.2	2.0	2.0	2 ± 0.2
Refractory	V	370	467	416 ± 14	297	296	317 ± 11

Highly Refractory	La	23.3	24.4	25 ± 1	14.4	14.9	15 ± 1
Highly Refractory	Pr	6.4	6.8	6.8 ± 0.3	5.1	5.3	5.34 ± 0.03 *
Highly Refractory	Nd	26.7	27.8	28 ± 2	23.3	24.0	25 ± 1.8
Highly Refractory	Sm	6.2	6.5	6.7 ± 0.3	5.8	6.1	6.2 ± 0.4
Highly Refractory	Ca	47926	47213	50900 ± 800	75911	78515	81700 ± 1200
Highly Refractory	Ti	12287	12808	13500 ± 300	14756	14685	16300 ± 200
Ultra Refractory	Gd	6.3	6.7	6.8 ± 0.3	5.9	6.1	6.3 ± 0.2
Ultra Refractory	Tb	1.0	1.0	1.07 ± 0.04	0.9	0.9	0.9
Ultra Refractory	Sc	31.6	31.7	33 ± 2	30.2	31.5	32 ± 1
Ultra Refractory	Y	33.6	35.7	37 ± 2	25.0	26.1	26 ± 2
Ultra Refractory	Hf	4.2	5.0	4.8 ± 0.2	4.1	4.6	4.1 ± 0.3

\* Literature values taken from Jochum et al. [22]

194

### 195 3.2 Timed digestion

196 One potential advantage LDHP has compared to traditional dissolution techniques for geological  
 197 samples is a drastic decrease in the dissolution time. Dissolving geological samples is an inexact  
 198 science, and the rate of, and total time for, dissolution is dependent on several parameters. These  
 199 include things like sample composition, such as organic or silica content, the temperature and  
 200 pressure of the dissolution, and of course the type, volume, and concentration of the acids used.  
 201 Dissolving a gram of basalt presents very different challenges to dissolving a gram of carbonate,  
 202 for instance. For reference, in the most efficient cases for traditional digestion for a basaltic  
 203 composition glass, the time would be on the order of days, not hours [e.g., 23]. In some cases, if  
 204 data from a sample is time sensitive—such as a forensic sample—rapid sample dissolution may  
 205 be desired. Similarly, if high throughput is needed, dissolution time is a crucial step in the  
 206 process. With rapidity in mind, we also tested the LDHP method to determine how quickly a  
 207 silica-rich geologic material could be dissolved.

208

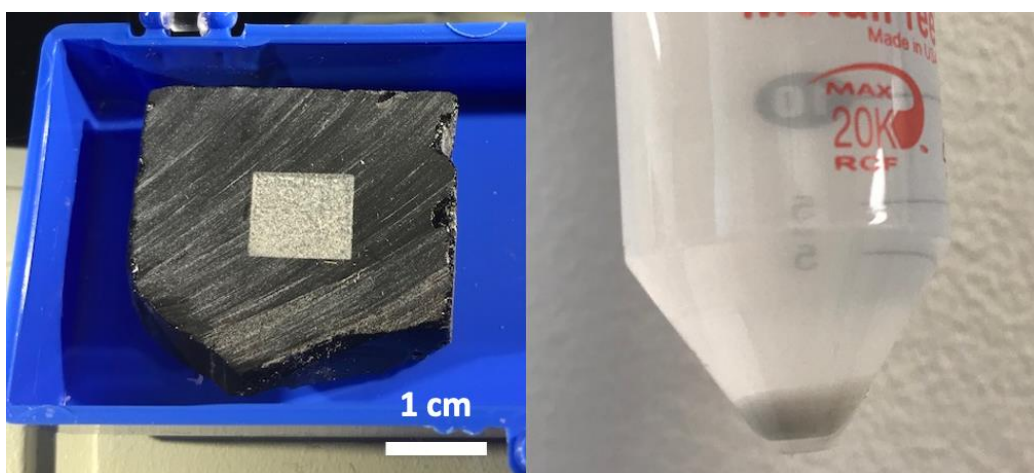
209 For this test, we used a piece of obsidian designated OBS-1, which was a Lake County, Oregon  
 210 obsidian sample purchased from Ward's Science, Inc. The sample OBS-1 was cut and prepared  
 211 by standard polishing techniques with up to 600 grit sandpaper, equivalent to ~ 10- $\mu$ m surface  
 212 roughness. OBS-1 was then weighed and then processed by LDHP in ~40 mL of 5 M nitric acid  
 213 in a cleaned glass beaker for two 10-minute intervals with a 10-minute break in between to allow  
 214 for cooling between laser firing sessions. After the second processing interval, OBS-1 was  
 215 removed from the glass beaker and rinsed with a few mL of MQ. The sample was dried and  
 216 weighed to determine the mass of material processed. The processed obsidian sample and  
 217 decanted supernatant and residues are shown in Figure 4. The solution and processed residue  
 218 were transferred into a 50 mL plastic centrifuge tube, where the sample was centrifuged for 5  
 219 minutes at 3000 rpm and subsequently split into solution and undissolved material. The  
 220 undissolved fines, along with ~3 mL of overlying solution was transferred to a 15 mL Savillex®  
 221 beaker for further processing. Concentrated HNO<sub>3</sub> (2mL), HF (2mL) and HCl (1mL) were  
 222 added, and then the sample was capped and heated at 140 °C. The sample was heated until  
 223 complete dissolution was observed. The step and time intervals are summarized in Table 3. A  
 224 total of 121 mg of material was removed during 20 minutes of laser processing. The cloudy color  
 225 of the supernatant in Figure 4 is a result of the suspended particles. Dissolution was considered  
 226 complete when the solution became transparent. This was confirmed by centrifuging the solution  
 227 a second time to ensure that no particulates gathered at the bottom of the tube. When both splits  
 228 of the sample were fully in solution, the splits were recombined. The total time to process the  
 229 sample and complete dissolution was 85 minutes, which translates into a rate of ~85 mg/hr for  
 230 this sample.

231  
232

Table 3. The laser assisted processing steps from sample to solution and associated time for each step.

Step	Time
Laser Processing	10 minutes
Cooldown	10 minutes
Laser Processing	10 minutes
Transfer to 50 mL centrifuge tube	5 minutes
Transit time	5 minutes
Acidification and heat	45 minutes
<b>Total Time</b>	<b>85 minutes</b>

233  
234



235  
236  
237

Figure 4. (left) The laser processed sample and (right) the decanted sample. Suspended particles in the supernatant cause the cloudy color and the collected residue is seen at the bottom.

238  
239

### 3.3 Potential areas of improvement

240 For this experiment, a baseline dissolution rate of ~85 mg/hr was achieved using ~40 mL of 5 M  
241 nitric acid and laser processing for 20 minutes. There are several additional parameters that can  
242 affect significant changes in this rate. As the laser processes the sample, part of the sample is  
243 dissolving but a significant fraction is also spalling off the surface creating an abundance of  
244 suspended particles. The suspended particles subsequently cause the focused laser beam to  
245 scatter, which significantly decreases the fluence of the laser. As shown in Figure 5, the fluence  
246 of the laser is coupled to the amount of material removed. Simply put, a lower fluence results in  
247 less material being removed, which is a decrease in efficiency of the process. As such, if the  
248 number of suspended particles decreases the effectiveness of the process, it will be important to  
249 innovate ways to decrease the number of suspended particles during LDHP to make it more  
250 effective.  
251

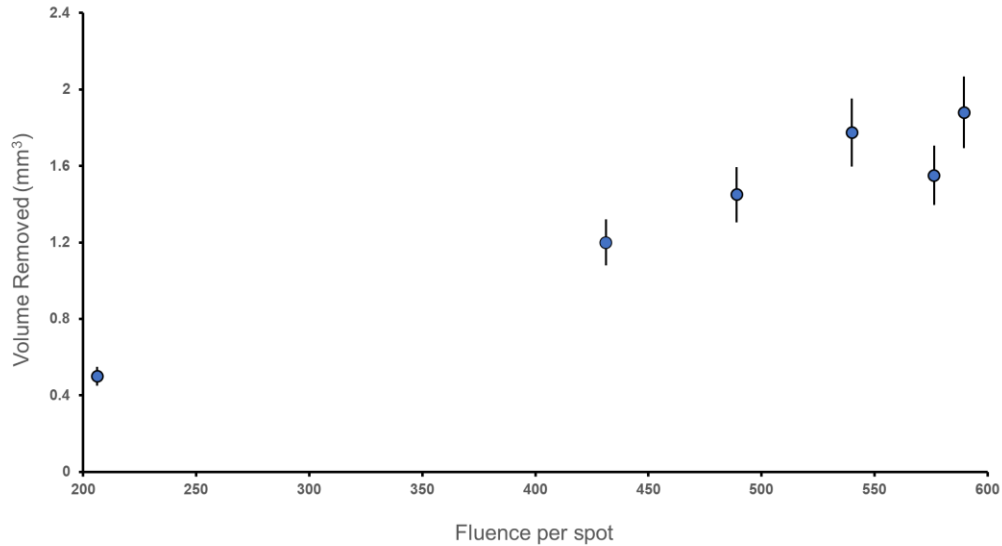


Figure 5. The total volume of obsidian removed by laser-assisted processing plotted against the total fluence per spot. The total fluence per spot was adjusted by increasing the power and keeping other laser parameters constant. Each point represents the material removal of a clean sample with no particle buildup prior to processing.

252  
253  
254  
255

256

257 Currently, our method of LDHP has been tested using MQ water and 5M nitric acid. It is  
258 possible that performing LDHP in more concentrated acid(s) would remove the need for the  
259 acidification step, but perhaps more importantly, the increased acid strength would cause more  
260 rapid dissolution of small particles, meaning fewer suspended particles present that could scatter  
261 the laser beam and decrease the fluence. Because the acidification step uses concentrated  
262 hydrofluoric acid (HF) and nitric acid, the laboratory must be set up to deal with such hazards.  
263 Additionally, LDHP processing currently takes place in a glass beaker, which is incompatible  
264 with HF. Typically, acid dissolutions that involve HF are performed in Teflon beakers, however,  
265 experiments proved these beakers unsuitable, as the laser quickly burns through Teflon. Thus,  
266 the suspension of particles during processing is a significant hurdle that must be overcome before  
267 adoption of this laser-assisted dissolution method can occur outside of specialized use cases such  
268 as removing a small section from a larger sample.

269

270 While overcoming the decreased processing efficiency due to suspended particles is a primary  
271 challenge, there are multiple avenues to increasing the overall processing and dissolution rate of  
272 a sample. The first avenue is to simply process the sample with the laser for a longer period.  
273 Adding additional laser processing steps may increase the amount of material removed by  
274 several times but the volume of acid or time needed to complete the dissolution after laser  
275 processing will remain nearly constant. Another option to increase the dissolution rate would be  
276 to increase the laser processing rate. Increasing the laser processing rate could be accomplished  
277 by increasing the beam area while delivering the same fluence per area. The beam area is  
278 increased by increasing the power of the laser while changing the focus so that the beam is  
279 larger. A larger beam area with the same intensity would increase the amount of material that can  
280 be processed in the same amount of time. Unfortunately, both increasing the processing time and  
281 increasing the beam area would lead to substantial increases in the number of particles  
282 suspended, decreasing the overall efficiency of the process. A third pathway to improving the  
283 dissolution rate is decrease the number of particles suspended in solution. Consequently, finding

284 a method to either remove or suppress the number of suspended particles will ultimately be the  
285 primary driver for increasing the dissolution rate.

286

#### 287 **4. Conclusions**

288 In this work, we show that laser-assisted dissolution does not produce elemental fractionation, as  
289 demonstrated for a range of elements with disparate geochemical behaviors—an important step  
290 establishing laser-assisted dissolution as a potential alternative to traditional acid digestion  
291 methods. Laser-assisted dissolution offers multiple potential advantages over traditional acid  
292 digestion, as a sample could be processed without direct contact to the sample (*i.e.*, without  
293 mechanical crushing), possibly eliminating sources of cross-contamination. Also, a selected  
294 subsample could be targeted and removed with greater ease using the laser-assisted method as  
295 opposed to other mechanical separation procedures. We have demonstrated that obsidian can be  
296 dissolved at a rate of at least 85 mg / hr using the described setup, with many potential  
297 improvements to come that could drastically increase this dissolution rate.

298

299 Overall, the use of laser-assisted dissolution has the potential to improve the timeliness, safety,  
300 and cleanliness of dissolving various, targeted materials. The areas in which this method could  
301 prove to be most helpful would be where samples need to be processed in a very short  
302 timeframe, such as a forensics sample. Similarly, in a situation where high-throughput of  
303 samples was a goal, laser-assisted dissolution could help streamline the process and remove one  
304 of the largest bottlenecks of sample processing.

305

#### 306 **Declarations**

307 The authors declare that they have no known competing financial interests or personal  
308 relationships that could have appeared to influence the work reported in this paper. This work  
309 does not involve any human or biological subjects.

310

#### 311 **Acknowledgements**

312 The authors would like to thank Dr. Corliss Sio for preparing the basalt samples. Lawrence  
313 Livermore National Laboratory is operated by Lawrence Livermore National Security, LLC, for  
314 the U.S. Department of Energy, National Nuclear Security Administration under Contract DE-  
315 AC52-07NA27344. This paper is LLNL-JRNL-825092.

316

#### 317 **References**

318

319 [1] R. Bock, “A Handbook of Decomposition Methods in Analytical Chemistry,” Blackie,  
320 Glasgow, 1979.

321

322 [2] W. M. Johnson, J. A. Maxwell, “Rock and Mineral Analysis,” Wiley, New York, N.Y.  
323 2<sup>nd</sup> ed., 1981.

324

325 [3] P. J. Potts, “A Handbook of Silicate Rock Analysis,” Blackie, London, 1987.

326

327 [4] Z. Sulcek, P. Povondra, “Methods of Decomposition in Inorganic Analysis,” CRC Press,  
328 Boca Raton, FL, 1989.

329

- 330 [5] G. A. Brennecka, L. E. Borg, M. Wadhwa (2014) “Insights into the Martian mantle: The  
331 age and isotopics of the meteorite fall Tissint,” *Meteorit Planet Sci*, **49**, 412-418.  
332
- 333 [6] G. Yang, (2007) “Laser ablation in liquids: Application in the synthesis of nanocrystals,”  
334 *Prog Mater Sci*, **52(4)**, 648-698.  
335
- 336 [7] H. Zeng, X. Du, S. Singh, S. Kulinich, S. Yang, J. He, W. Cai, (2012) “Nanomaterials via  
337 Laser Ablation/Irradiation in Liquid: A Review,” *Adv Funct Mater*, **22(7)**, 1333-1353.  
338
- 339 [8] J. Xiao, P. Liu, C. Wang, G. Yang, (2017) “External field-assisted laser ablation in liquid:  
340 An efficient strategy for nanocrystal synthesis and nanostructure assembly,” *Prog Mater Sci*,  
341 **87**, 140-220.  
342
- 343 [9] D. Zhang, B. Gökce, S. Barcikowski, (2017) “Laser Synthesis and Processing of  
344 Colloids: Fundamentals and Applications,” *Chem Rev*, **117**, 3990-4103.  
345
- 346 [10] R. Dingus, R. Scammon, “Ablation of material by front surface spallation,” *Laser*  
347 *Ablation Mechanisms and Applications: Proceedings of a Workshop Held in Oak Ridge, TN,*  
348 *USA 8-10 April 1991*, **389**, 180, 1991.  
349
- 350 [11] M. Yoshimura, K. Byrappa, (2008) “Hydrothermal processing of materials: past,  
351 present, and future,” *J Mater Sci*, **43**, 2085-2103.  
352
- 353 [12] R. Mariella, B. Mills, (2018) “Laser-driven hydrothermal processing: a new efficient  
354 technique to effect separation of silica from other oxides for analysis,” *Laser Phys Lett*, **15**.  
355
- 356 [13] S. A. Wilson, “The collection, preparation and testing of USGS reference material BCR-  
357 2,” US Geological Survey, Open File Report, 1997.  
358
- 359 [14] S. A. Wilson, “Data compilation for USGS reference material BHVO-2, Hawaiian  
360 Basalt,” US Geological Survey, Open-file Report, 1997.  
361
- 362 [15] R. Mariella, A. Rubenchik, M. Norton, G. Donohue, (2013) “Laser comminution of  
363 submerged samples,” *J Appl Phys*, **114**, 14904-1.  
364
- 365 [16] R. Mariella, A. Rubenchik, E. Fong, M. Norton, W. Hollingsworth, J. Clarkson, H.  
366 Johnsen, D. L. Osborn, (2017) “Laser-driven hydrothermal process studied with excimer laser  
367 pulses,” *J Appl Phys*, **122**, 75104-1.  
368
- 369 [17] S. Menon, A. Camargo, C. Wu, R. Mariella, C. Luhrs (2017) “Characterization of particles  
370 created by laser-driven hydrothermal processing,” *Mater Charact*, **133**, 1.  
371
- 372 [18] J. Wimpenny, N. Marks, K. Knight, J. M. Rollison, L. E. Borg, G. Eppich, J. Badro, F. J.  
373 Ryerson, M. Sanborn, M. H. Huyskens, Q. Z. Yin, (2019) “Experimental determination of Zn  
374 isotope fractionation during evaporative loss at extreme temperatures,” *Geochim Cosmochim*  
375 *Ac*, **259**, 391-411.

- 376  
377 [19] J. Wimpenny, N. Marks, K. Knight, L. E. Borg, J. Badro, F. J. Ryerson, (2020)  
378 “Constraining the behavior of gallium isotopes during evaporation at extreme temperatures,”  
379 *Geochim Cosmochim Ac*, **286**, 54-71.  
380  
381 [20] L. E. Borg, W. S. Cassata, J. Wimpenny, A. M. Gaffney, C. K. Shearer, (2020) “The  
382 formation and evolution of the Moon’s crust inferred from the Sm-Nd isotopic systematics of  
383 highlands rocks,” *Geochim Cosmochim Ac*, **290**, 312-332.  
384  
385 [21] K. Lodders, (2003) “Solar system abundances and condensation temperatures of the  
386 elements,” *Astrophys J*, **591**, 1220-1247.  
387  
388 [22] K. P. Jochum, U. Weis, B. Schwager, B. Stoll, S. A. Wilson, G. H. Haug, M. O.  
389 Andreae, J. Enzweiler, (2016) “Reference values following ISO guidelines for frequently  
390 requested rock reference materials,” *Geostand Geoanal Res*, **40**, 333-350.  
391  
392 [23] I. Raczek, B. Stoll, A. W. Hofmann, K. P. Jochum (2001) “High-Precision Trace  
393 Element Data for the USGS Reference Materials BCR-1, BCR-2, BHVO-1, BHVO-2, AGV-  
394 1, AGV-2, DTS-1, DTS-2, GSP-1 and GSP-2 by ID-TIMS and MIC-SSMS,” *Geostandard*  
395 *Newslett*, **25**, 77-86.  
396

## Figures

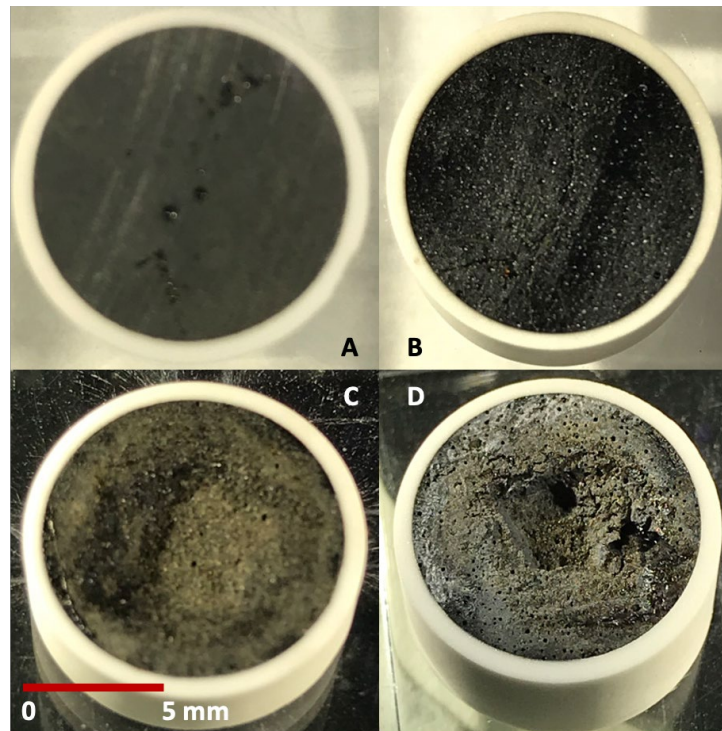


*Figure 1. The geostandard samples BHVO-2 and BCR-2 prior to laser processing are shown in (A) and (B) respectively. The post-processed BHVO-2 and BCR-2 samples are shown in (C) and (D) respectively. Approximately 12 mg was processed and removed from the BCR-2 sample and 15 mg was processed and removed from the BHVO-2 sample.*

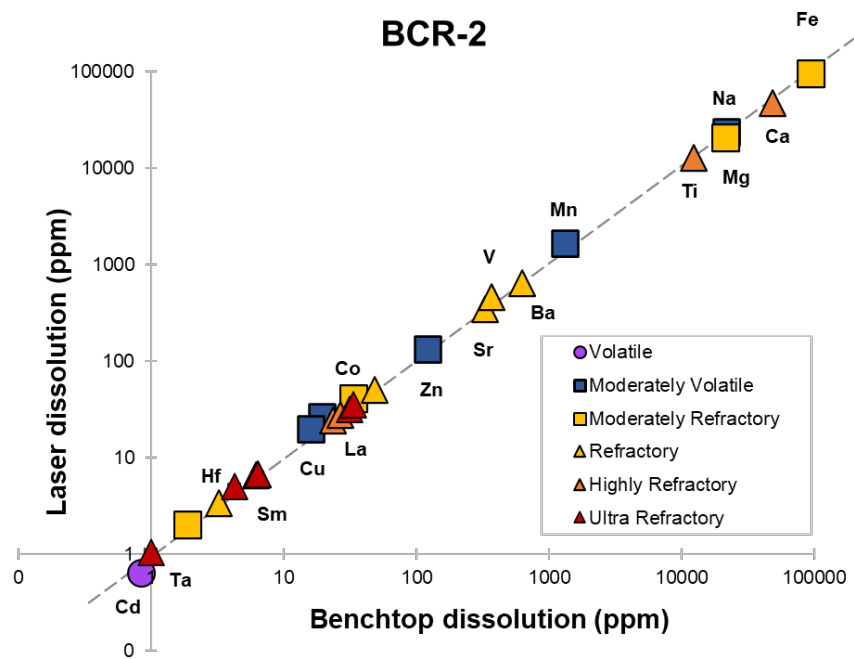


Figure 3: A comparison of elemental concentrations obtained by a traditional benchtop dissolution and laser assisted dissolution of BCR-2. The dashed gray line is a 1:1 line for reference. For clarity, not all elements are labeled. Uncertainties of 10% are smaller than the symbols.

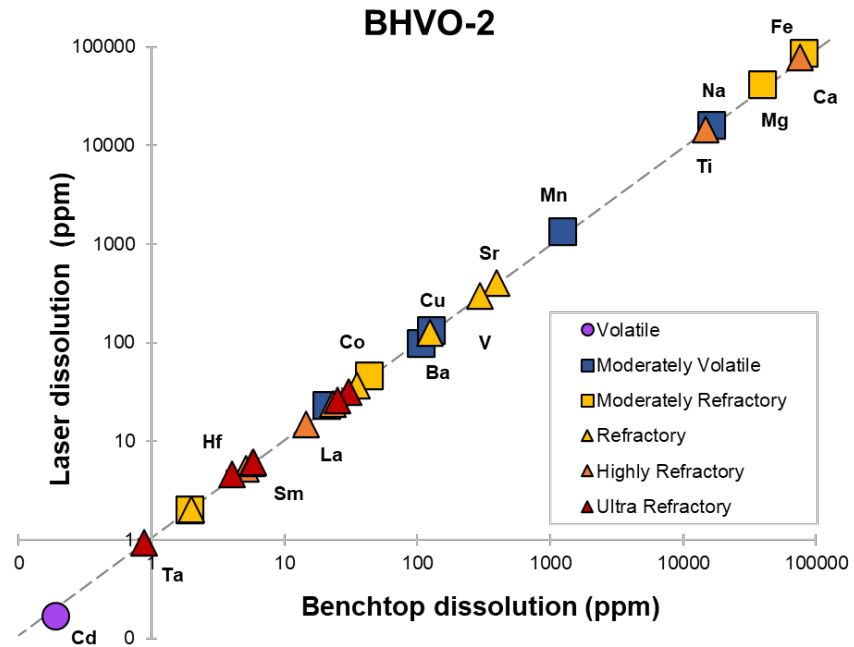


Figure 4. A comparison of elemental concentrations obtained by both a traditional benchtop dissolution and laser assisted dissolution of BHVO-2. The dashed gray line is a 1:1 line for reference. For clarity, not all elements are labeled. Uncertainties of 10% are smaller than the symbols.

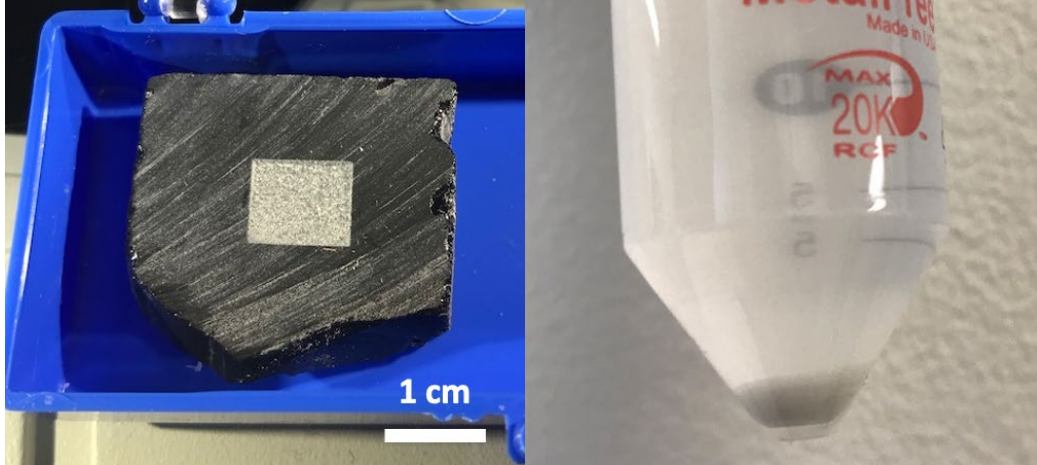
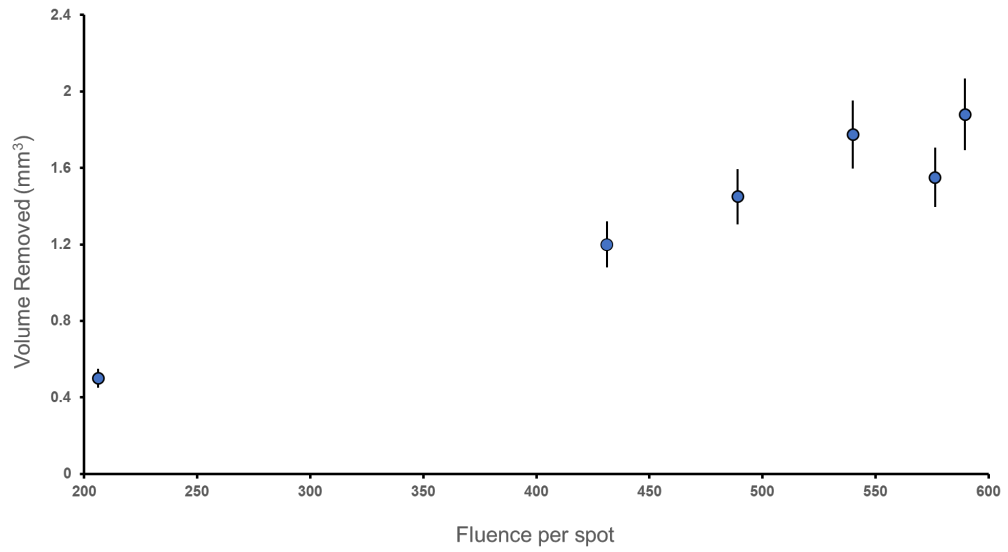


Figure 5. (left) The laser processed sample and (right) the decanted sample. Suspended particles in the supernatant cause the cloudy color and the collected residue is seen at the bottom.



*Figure 6. The total volume of obsidian removed by laser-assisted processing plotted against the total fluence per spot. The total fluence per spot was adjusted by increasing the power and keeping other laser parameters constant. Each point represents the material removal of a clean sample with no particle buildup prior to processing.*